Proceedings of the
47th IEEE Conference on Decision and Control
Cancun, Mexico, Dec. 9-11, 2008



# Mechatronic Suspension Design and Its Applications to Vehicle Suspension Control

Fu-Cheng Wang* and Hsiang-An Chan

***Abstract*—This paper proposes the design of a novel mechatronic suspension strut, and investigates the performance benefits of vehicle suspension systems employing it. The proposed mechatronic suspension strut consists of a ball-screw inerter and permanent magnet electric machinery (PMEM), such that the system impedance can be realized through the combination of mechanical and electrical networks. Furthermore, we apply the mechatronic strut to vehicle suspension control, and discuss performance improvement. From the results, the proposed mechatronic suspension is deemed effective.**

## I. Introduction

The analogy between mechanical and electrical systems is well known [1]. For example, in the "force-current analogy", the physical characteristics of mass, damping and spring correspond to the electrical characteristics of capacitance, resistance and inductance, respectively. However, the mass element fails to be a genuine two-terminal network element in that one terminal of the mass is always connected to the ground. Therefore, in order to compare a conventional mass element with an electrical element, the corresponding electrical element must have one terminal connected to the ground. Nevertheless, this requirement limits the freedom or flexibility in designing mechanical systems, since not all passive impedances can be mechanically realized by masses, dampers and springs. To solve the problem, the inerter was proposed as an ideal mechanical two-port element to substitute for the mass element in the mechanical/electrical analogy, with the following defining equation:

$$F = b\frac{d(v_2 - v_1)}{dt}, \qquad (1)$$

in which $F$ is the applied force and $b$ represents the inertance of the system, while $v_1$ and $v_2$ are the velocities of the two terminals [1]. Consequently, all passive mechanical networks, which can be realized by springs, dampers and inerters, are able to be used to improve system performance.

The inerter was applied to vehicle suspension systems in [2], where suspension layouts with inerters were optimized for some performance measures. The results showed that system performance can be significantly improved by inerters. In [3], the optimization was further carried out by the Linear Matrix Inequalities (LMI) method, and the resulting passive networks were synthesized by Bott-Duffin realization. It was illustrated that system performance can be further improved by allowing higher order passive impedance. However, the network synthesis for high-order impedance can be very complicated and hard to realize mechanically. Therefore, in this paper we propose a novel mechatronic suspension strut, which is composed of a ball-screw inerter and permanent magnet electric machinery (PMEM). It is shown that the system impedance can be realized through the combination of mechanical and electrical networks, such that the high-order transfer functions from LMI approaches can be easily realized by electrical circuits.

Behrens et al. [4, 5] propose a broadband active/passive shunt technique to reduce structural vibrations effectively using piezoelectric and electromagnetic transducers. Paulitsch et al. [6] investigated the vibration reduction of a clamped plate using a self-sensing, electro-dynamic actuator, and indicated that self-sensing active/passive vibration damping is advantageous if external sensors cannot be collocated with the actuators or are too costly. This paper combines these ideas with the use of a ball-screw inerter, and presents the mechatronic suspension design using the perfect analogy between mechanical and electrical systems. The paper is arranged as follows: in Section 2, we introduce the mechatronic suspension design and construct a block diagram to represent the system structure. In Section 3, the proposed mechatronic strut is applied to vehicle suspension control for performance optimization. In Section 4, we discuss the performance benefits of the suspension system employing the mechatronic strut. In Section 5, the properties of the mechatronic strut are verified experimentally. Finally, we draw some conclusions in Section 6.

## II. The Mechatronic Suspension Structure

In this section, we will introduce the mechatronic suspension strut, which composes of a ball-screw inerter and PMEM, as shown in Figure 1. The design structure of the strut is illustrated in Figure 2.


Figure 1. The prototype of a mechatronic suspension strut.

Manuscript received on March 8, 2008. This work was supported in part by the National Science Council of Taiwan under Grant 95-2218-E-002-030.

Fu-Cheng Wang is with the Mechanical Engineering Department of National Taiwan University, No.1, Sec. 4, Roosevelt Road, Taipei 10617, Taiwan. (phone: +886-2-33662680; fax: +886-2-23631755; e-mail: fcw@ntu.edu.tw).

Hsiang-An Chan is with the Mechanical Engineering Department of National Taiwan University, Taiwan. (e-mail: cardiel740@yahoo.com).

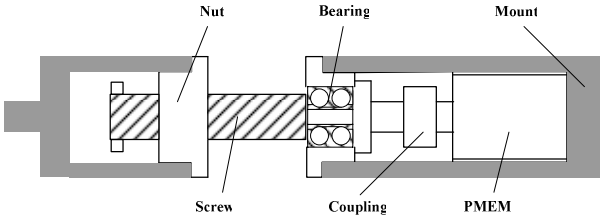

Figure 2. The design structure.

### A. The Ball-Screw Inerter

Inerters can be mechanically realized by various methods, such as the rack-and-pinion inerter [2] and the ball-screw inerter [7, 8], which can convert the linear movement into rotational movement and achieve the inerter functions. The dynamic equations of a ball-screw inerter are as follows:

$$\omega = (2\pi / P)v\,, \tag{1}$$

$$F = (2\pi / P)T\,, \tag{2}$$

in which $v$ is the relative velocity of the two terminals and $\omega$ is the angular velocity of the screw, while $F$ and $T$ are the applied force on the terminals and the reaction torque on the screw, respectively, and $P$ is the pitch of the ball-screw. Furthermore, the torque $T$ and angular velocity $\omega$ are related as follows:

$$T = J(d\omega / dt)\,, \tag{3}$$

where $J$ is the mass moment of inertia of the ball-screw inerter. Substituting (2-3) into (1), one can obtain the following inerter equation:

$$F = (2\pi / P)^2 J(dv / dt) = b \cdot a\,, \tag{4}$$

in which $b$ is the system inertance and $a$ is the relative acceleration of the two terminals. It is note that the system inertance $b$ can be easily adjusted by tuning the attached flywheel.

### B. The Permanent Magnet Electric Machinery (PMEM)

The ball-screw inerter is connected with a PMEM, such that the linear movement across two terminals can generate corresponding voltage and thus the designed force through the construction of electrical networks. The working principles of a PMEM are illustrated in Figure 3, in which the internal magnetic flux $\Phi$ is constant and the armature of the PMEM is regarded as a resistor $R_a$ in series with an inductor $L_a$. Furthermore, $Z_e$ presents the impedance of external electrical circuits, while $J_m$ and $B_m$ present the mass moment of inertia and the damping coefficient of the PMEM, respectively.

Firstly, supposing the shaft rotates with angular velocity $\omega$, the inductive voltage $V_g$ of the PMEM can be represented as:

$$V_g = k_e \cdot \omega\,, \tag{5}$$

where $k_e$ is the inductive voltage constant. Assuming the armature current is $I_a$, the corresponding inductive torque $T_e$ of the PMEM is:

$$T_e = k_t \cdot I_a\,, \tag{6}$$

in which $k_t$ is the inductive torque constant. Note that $k_e$ and $k_t$ are in the units of Vs/rad and Nm/A, respectively, and are determined by the internal magnetic flux $\Phi$, the number of the armature coils and poles of the PMEM.

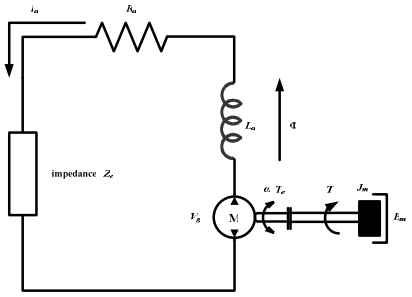

Figure 3. The PMEM model.

The system admittance of Figure 3 can be taken as follows:

$$\frac{\hat{I}_a(s)}{\hat{V}_g(s)} = \frac{1}{R_a + sL_a + Z_e(s)}\,, \tag{7}$$

in which " ˆ " represents the Laplace transform of the corresponding variables. The dynamic equation of the mechanical part can be presented as:

$$J_m \frac{d\omega}{dt} = T - T_e - B_m\omega\,, \tag{8}$$

where $T$ is the external torque to the PMEM. Taking the Laplace transform of (8) gives:

$$J_m s\hat{\omega}(s) = \hat{T}(s) - \hat{T}_e(s) - B_m\hat{\omega}(s)\,. \tag{9}$$

Combining the ball-screw inerter with the PMEM, (9) can be modified as:

$$(J_m + J)s\hat{\omega}(s) = \hat{T}(s) - \hat{T}_e(s) - B_m\hat{\omega}(s)\,. \tag{10}$$

Taking the Laplace transform of (1-2, 5-6), the equations are represented as:

$$\hat{\omega}(s) = (2\pi / P)\hat{v}(s)\,, \tag{11}$$

$$\hat{F}(s) = (2\pi / P)\hat{T}(s)\,, \tag{12}$$

$$\hat{V}_g(s) = k_e\hat{\omega}(s)\,, \tag{13}$$

$$\hat{T}_e(s) = k_t\hat{I}_a(s)\,. \tag{14}$$

By substituting (11, 12, 14) into (10), one can obtain the following equation:

$$(J_m + J)s(\frac{2\pi}{P})\hat{v}(s) = (\frac{P}{2\pi})\hat{F}(s) - k_t\hat{I}_a(s) - B_m(\frac{2\pi}{P})\hat{v}(s)\cdot \tag{15}$$

Now substituting (7, 11, 13) into (15) gives:

$$\frac{\hat{F}(s)}{\hat{v}(s)} = (\frac{2\pi}{P})^2\left[(J_m + J)s + B_m + \frac{k_t k_e}{R_a + sL_a + Z_e(s)}\right], \tag{16}$$

which is the admittance of the mechatronic suspension strut, and can be represented by a block diagram, as shown in Figure 4. We now define the following parameters:

$$b_m = (2\pi / P)^2(J_m + J)\,,$$

$$c_m = (2\pi / P)^2 B_m\,,$$

$$K_m = (2\pi / P)^2 k_t k_e\,,$$

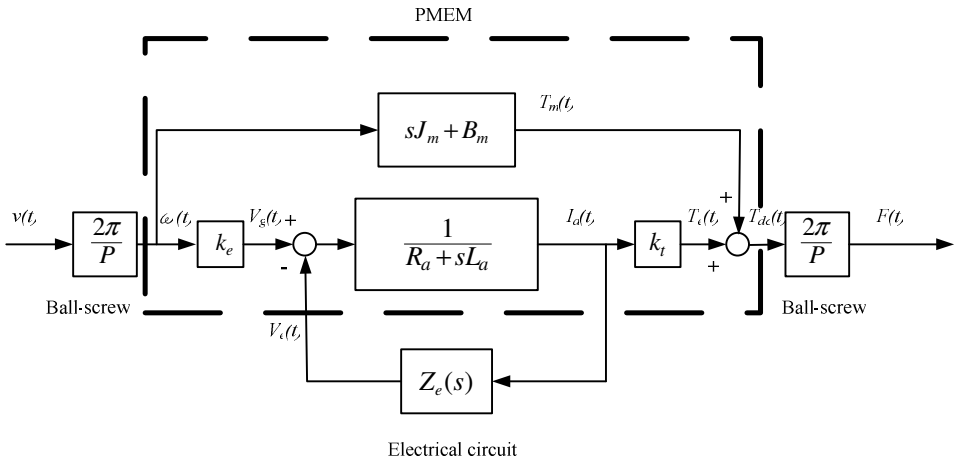


Figure 4. Block diagram of mechatronic suspension system.

in which $b_m$, $c_m$ and $K_m$ are the inertance, damping rate and admittance gain of the mechatronic suspension, respectively. Therefore, (16) can be rewritten as:

$$\frac{\hat{F}(s)}{\hat{v}(s)} = b_m s + c_m + \frac{K_m}{R_a + sL_a + Z_e(s)}. \qquad (17)$$

The right-hand side of (17) can be divided into two parts. The first part, $b_m s + c_m$, can be considered as the mechanical inerter and damper of the mechatronic suspension system. The second part $K_m / (R_a + sL_a + Z_e(s))$ can be regarded as the admittance of electronic circuits of the mechatronic suspension system. Using the analogy between mechanical and electrical networks, (17) can be represented as a mechanical system as shown in Figure 5.

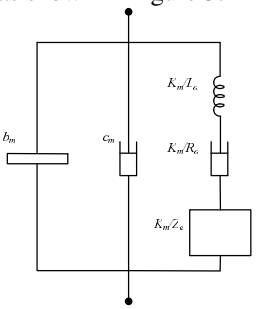


Figure 5. The ideal mechatronic suspension model.

## III. Vehicle Suspension Models

In this section, we introduce a quarter-car model and six suspension layouts, and discuss the performance benefits of vehicle suspensions employing mechatronic suspension layouts using two proposed performance measures.

### A. The Quarter-Car Model

A quarter-car model is illustrated in Figure 6, with dynamic equations as follows:

$$m_s \ddot{z}_s = F_s - u, \qquad (18)$$

$$m_m \ddot{z}_m = u - F_r, \qquad (19)$$

where $F_r = k_t(z_u - z_r)$ is the tyre force, and $u$ is the suspension force, which depends on the applied suspension layouts as in the following:

$$\hat{u}(s) = \hat{Q}(s) \cdot s(\hat{z}_s - \hat{z}_b),$$

in which $\hat{Q}(s)$ is the admittance of the suspension strut.

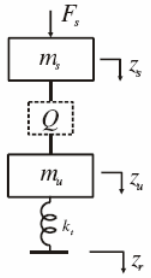


Figure 6. The quarter-car model.

### B. The Suspension Layouts

Six basic suspension layouts are considered for analysis, as shown in Figure 7. We note that S1 is the traditional suspension, while S2 is a basic parallel arrangement and S3 is a basic serial arrangement with inerter. For comparison, LMIS1 is the mechatronic suspension in parallel with a spring, while LMIS2 and LMIS3 use a stiff spring and a parallel spring/damper, respectively, in serial with the mechatronic suspension. Applying the suspension struts to the quarter-car model, the suspension forces can be represented in the following:

S1: $\hat{u} = (k + c \cdot s)(\hat{z}_s - \hat{z}_u)$

S2: $\hat{u} = (k + c \cdot s + b \cdot s^2)(\hat{z}_s - \hat{z}_u)$

S3: $\hat{u} = (k + \frac{b \cdot c \cdot s^2}{b \cdot s + c})(\hat{z}_s - \hat{z}_u)$

LMIS1: $\hat{u} = (k + Y_{ms})(\hat{z}_s - \hat{z}_u)$

LMIS2: $\hat{u} = (k + \frac{k_b \cdot Y_{ms}}{k_b + Y_{ms}})(\hat{z}_s - \hat{z}_u)$

LMIS3: $\hat{u} = (k + \frac{(k_b + c_b \cdot s) \cdot Y_{ms}}{k_b + c_b \cdot s + Y_{ms}})(\hat{z}_s - \hat{z}_u)$

where $Y_{ms} = (b_m s^2 + c_m s + \frac{K_m s}{R_a + s \cdot L_a + Z_e})$ is the admittance of the mechatronic suspension strut.

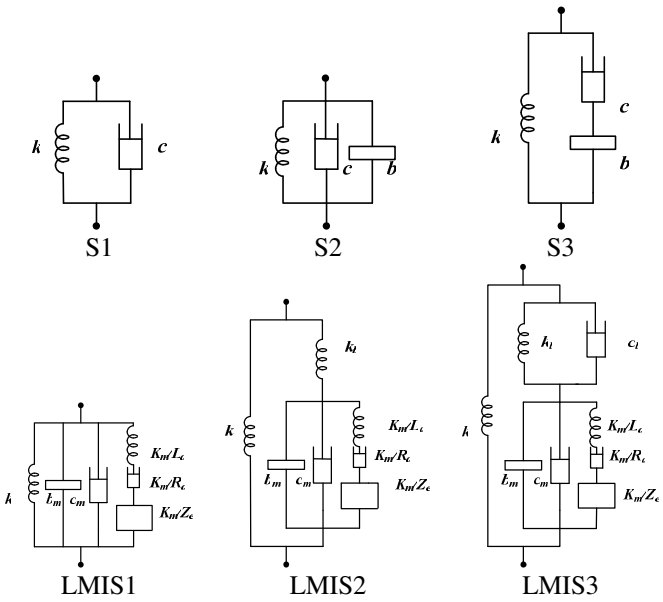


Figure 7. Suspension layouts

### C. *The Performance Measures*

To illustrate the performance benefits, two performance indexes defined as follows [2] are selected:

1). $J_1$ (ride comfort)

$$J_1 = 2\pi\sqrt{(V\kappa)}\left\|T_{\hat{z}_r\to\hat{z}_s}\right\|_2 = 2\pi\sqrt{(V\kappa)}\left\|sT_{\hat{z}_r\to\hat{z}_s}\right\|_2, \qquad (20)$$

2). $J_3$ (dynamic tyre loads)

$$J_3 = 2\pi\sqrt{(V\kappa)}\left\|\frac{1}{s}T_{\hat{z}_r\to k_t(\hat{z}_u-\hat{z}_r)}\right\|_2, \qquad (21)$$

where $V$ represents the driving velocity, while $\kappa$ is the road roughness parameter. And $\boldsymbol{T}_{\hat{z}_r\to\hat{z}_s}$ is the transfer function from $\hat{z}_r$ to $\hat{z}_s$ and $\|T\|_2$ is the $H_2$ norm of $T$. The parameters of $V = 25$ m/s and $\kappa = 5\times10^{-7}$ m$^3$cycle$^{-1}$ are set for performance analyses.

## IV. Performance Benefits of the Suspension System

Applying the aforementioned suspension layouts, the performance measures $J_1$ and $J_3$ are optimized to illustrate the performance benefits. Given a fixed suspension stiffness $k$, we optimize the parameters $b$ and $c$ for layouts S1, S2 and S3 [2], and optimize over all passive transfer functions using LMI approaches [3] for layouts LMIS1, LMIS2 and LMIS3. The resulting impedances $Z_e$ of LMIS1, LMIS2 and LMIS3 can then be realized by either the Bott-Duffin or Brune methods [3]. The following parameters are used for numerical simulations: $m_s$=250kg, $m_u$=35kg, $k_t$=150kN/m, $R_a$=2.3Ω, $L_a$=0.7mH, $K_m$=7056 VNs/A/m. The static stiffness is set in the range 10-120kN/m.

### A. *The Optimization of $J_1$*

The results of $J_1$ optimization are shown in Figure 8, where the impedance $Z_e$ of LMIS1~LMIS3 are set as 1st and 2nd orders. It is noted that the LMIS1 achieves better performance benefits than the fixed structures for soft stiffness settings. On the other hand, LMIS2 achieves similar results to LMIS1, and hence is not illustrated in the plots. Finally, LMIS3 is the best among the six layouts in the considered stiffness range. From the previous studies [2, 7, 8], we note that inerter is particularly useful for stiff systems, but fails to improve much performance for soft systems. On the contrary, the proposed mechatronic suspension struts can significantly improve the suspension performance for both soft and stiff systems.

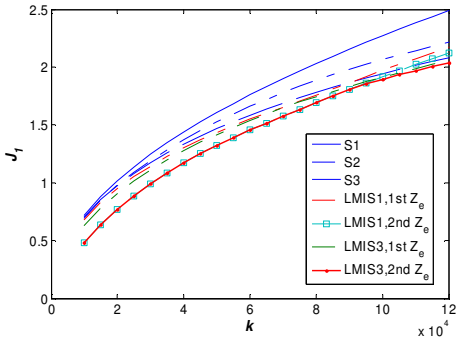


(a) Optimal $J_1$.

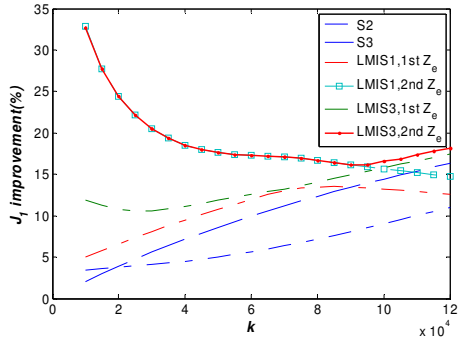


(b) % improvement of $J_1$.

Figure 8. Optimization of $J_1$.

Table 1. Optimization of $J_1$ with $k_s$=50k N/m.
($c_i$ in units of Ns/m, $b_i$ in units of kg)

| Layout | $J_1$ | % impro | $b$ ($b_m$) | $c$ ($c_m$) | $k_b$ | $c_b$ |
|---|---|---|---|---|---|---|
| S1 | 1.6066 | - | - | 2179 | - | - |
| S2 | 1.5259 | 5.023 | 22 | 1966 | - | - |
| S3 | 1.4684 | 8.602 | 314 | 2609 | - | - |
| LMIS1,1st | 1.4335 | 10.774 | 15 | 0 | - | - |
| LMIS1,2nd | 1.3239 | 17.596 | 28 | 0 | - | - |
| LMIS3,1st | 1.4164 | 11.839 | 32 | 0 | 55 | 3328 |
| LMIS3,2nd | 1.3239 | 17.596 | 28 | 0 | 2979k | 11906k |

Setting the stiffness as $k$=50k N/m, the optimization results for $J_1$ is illustrated in Table 1, with the corresponding electrical impedance as follows:

(a) LMIS1

1. $Z_e^{1st} = \dfrac{0.86s + 20.86}{s + 3.1\times10^{-7}}$

2. $Z_e^{2nd} = \dfrac{6.745\times10^5 s^2 + 2.34\times10^6 s + 2.214\times10^8}{s^2 + 6.252\times10^6 s + 44.18}$

(b) LMIS3

1. $Z_e^{1st} = \dfrac{1.798\times10^{-12} s + 35.89}{s + 1.42\times10^{-7}}$

2. $Z_e^{2nd} = \dfrac{1.665\times10^5 s^2 + 5.776\times10^5 s + 5.466\times10^7}{s^2 + 1.544\times10^6 s + 0.3419}$

### B. *The Optimization of $J_3$*

Similarly, the results of $J_3$ optimization are shown in Figure 9, where the impedance $Z_e$ of LMIS2 and LMIS3 are set as 1st and 2nd orders. Here LMIS1 is not discussed because it does not achieve better performance than LMIS2. From the results, the LMIS2 achieves better performance benefits than the fixed structures for soft stiffness settings, and LMIS3 is the best among the six layouts in the considered stiffness range. To conclude, the proposed mechatronic suspension struts can significantly improve the suspension performance for both soft and stiff systems.

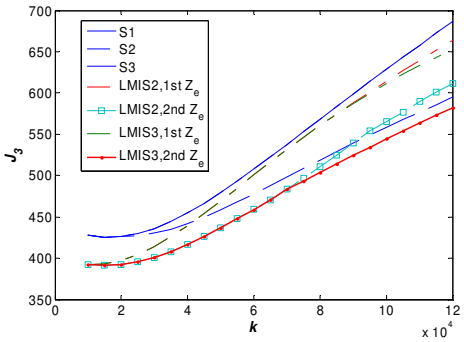


(a) Optimal $J_3$.

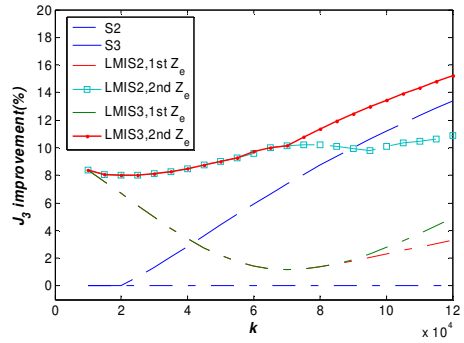


(b) % improvement of $J_3$.

Figure 9. Optimization of $J_3$.

Setting the stiffness as $k_s$=50k N/m, the corresponding parameter settings for $J_3$ optimization are illustrated in Table 2, with the first- and second-order passive electrical impedances of LMIS2 and LMIS3 as follows:

(a) LMIS2

1. $Z_e^{1st} = \dfrac{0.01529s + 3.797\times10^7}{s + 4.387\times10^7}$

2. $Z_e^{2nd} = \dfrac{600.3s^2 + 1.555\times10^4 s + 7.598\times10^5}{s^2 + 2.72\times10^4 s + 0.006011}$

(b) LMIS3

1. $Z_e^{1st} = \dfrac{9.468\times10^{-6} s + 1.894\times10^6}{s + 2.188\times10^6}$

2. $Z_e^{2nd} = \dfrac{2726s^2 + 7.06\times10^4 s + 3.45\times10^6}{s^2 + 1.235\times10^5 s + 0.6756}$

Table 2. Optimization of $J_3$ with $k_s$=50k N/m.
($c_i$ in units of Ns/m, $b_i$ in units of kg)

| Layout | $J_3$ | % improv | $b$ ($b_m$) | $c$ ($c_m$) | $k_b$ | $c_b$ |
|---|---|---|---|---|---|---|
| S1 | 479.6511 | - | - | 2392 | - | - |
| S2 | 479.6511 | 0 | 0 | 2392 | - | - |
| S3 | 458.4278 | 4.425 | 388 | 2618 | - | - |
| LMIS2,1st | 469.0712 | 2.208 | 21 | 0 | 231 | - |
| LMIS2,2nd | 436.5300 | 8.990 | 26 | 0 | 187 | - |
| LMIS3,1st | 469.0712 | 2.208 | 21 | 0 | 231 | 0 |
| LMIS3,2nd | 436.5300 | 8.990 | 25 | 0 | 186 | 0 |

## V. Experimental Results

In this section, we construct a mechatronic suspension strut, and use a testing platform to verify its properties. Considering the system nonlinearities, such as the twisting effect, backlash and friction, a nonlinear model of the system is illustrated in Figure 10 [7], where $K_s$, $C_s$ represent the elastic effect, while $\varepsilon$ and $f$ represent the backlash and friction, respectively. The model is built in Matlab/Simulink™, such that the simulation results can then be compared with the experimental data to determine the corresponding parameters.

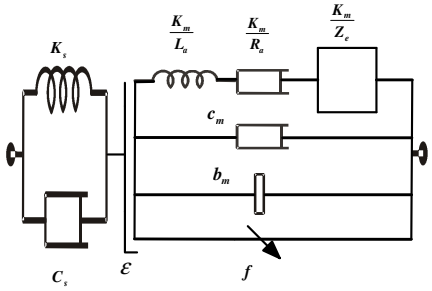


Figure 10. Nonlinear mechatronic suspension model.

A motion platform is shown in Figure 11 which has one degree of freedom and is driven by a servo motor to control the displacement of the suspension strut. The force of the device is measured by an S-type load cell with a maximum load of 100 kg and the resolution of 0.02 kg, while the displacement is measured by a position encoder with accuracy of 1 μm. Both the force and displacement signals are transferred to a LabView™ program to control the movement of the platform and to record the data.

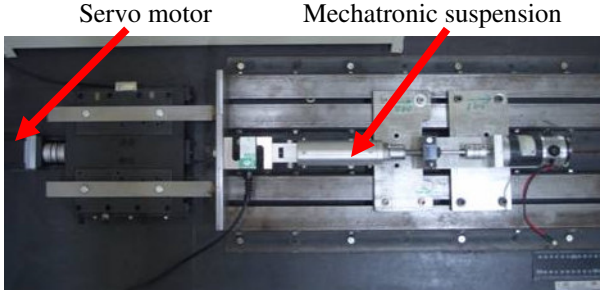


Figure 11. The motion platform.

Using the methods introduced in [7], the following parameters are evaluated from the comparison of the

experimental and theoretical data: $K_s$ = 110 kN/m, $C_s$ = 1040 Ns/m, $b_m$ =18.5 kg, $c_m$ =80 Ns/m, $f$ = 15 N and $\mathcal{E}$ = 0. It is noted that $\mathcal{E}$ is actually zero since the backlash of a ball-screw can normally be eliminated in the manufacturing process using preloading methods. To compare the frequency responses (from strut displacements to forces) of the experimental and theoretical models, we set some additional parameters, $R_a$=4.34Ω, $L_a$=6.76mH and $K_m$=7011VNs/A/m, from the experimental results.

The verification of the mechatronic strut was carried out in two steps. First, we tested the open-loop situation ( $Z_e = \infty$ ), as illustrated in Figure 12.

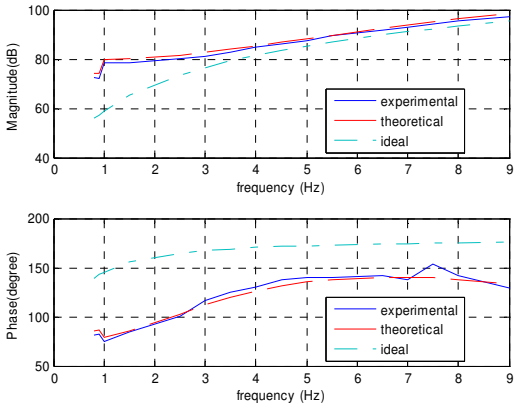


Figure 12. Frequency responses when $Z_e = \infty$.

Secondly, we used the following first-order and second-order electrical impedances:

$$Z_e^{1st} = \frac{352.1992(s+1079)}{s+1.445\times10^6},$$

$$Z_e^{2nd} = \frac{583.4812(s+473.9)(s+6300)}{(s+6575)(s+2145)}.$$

The results are shown in Figures 13 and 14, respectively. In Figures 12~14, 'ideal' means simulation of the mechatronic suspension without nonlinearities, and 'theoretical' means simulation of the mechatronic suspension with nonlinearities, while 'experimental' represents the experimental data. From the results, the proposed mechatronic suspension did achieve the designed properties.

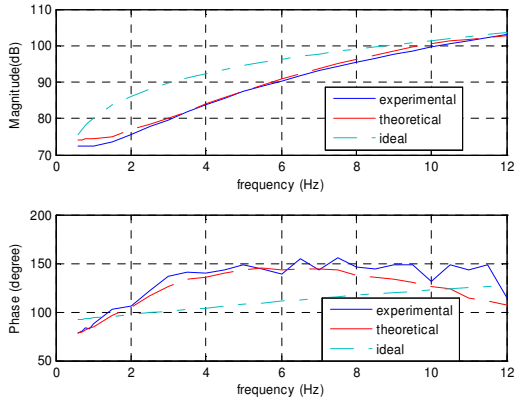


Figure 13. Frequency responses when $Z_e = Z_e^{1st}$.

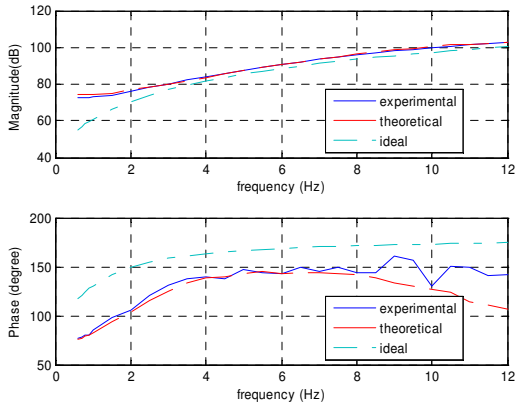


Figure 14. Frequency responses when $Z_e = Z_e^{2nd}$.

## VI. Conclusion

In this paper, we have proposed a novel mechatronic suspension design and applied it to vehicle suspension control. The mechatronic suspension strut consists of a ball-screw inerter and PMEM, such that the desired system impedance/admittance can be easily realized by the combination of mechanical and electrical networks. The applications to vehicle suspension systems showed that the proposed design can significantly improve the performance, especially for soft systems where the traditional inerter structures cannot achieve much performance improvement. Furthermore, the designed mechatronic suspension strut was tested to verify its properties. From the results, the proposed mechatronic suspension strut is deemed effective.

## References

[1]. M.C. Smith, *Synthesis of Mechanical Networks: The Inerter.* IEEE Transactions on Automatic Control, 47 (2002), pp. 1648–1662.

[2]. M.C. Smith and F.C. Wang, *Performance Benefits in Passive Vehicle Suspensions Employing Inerters.* Vehicle System Dynamics 42 (4): 235-257, OCT 2004.

[3]. C. Papageorgiou and M.C. Smith, *Positive Real Synthesis Using Matrix Inequalities for Mechanical Networks: Application to Vehicle Suspension.* IEEE Transaction on Control Systems Technology, 14 (2006), pp. 423–435.

[4]. S. Behrens, A.J. Fleming and S.O.R, Moheimani, *A broadband controller for shunt piezoelectric damping of structural vibration,* Smart Materials and Structures, Volume 12, Number 1, pp.36-48, February 2003.

[5]. S. Behrens, A.J. Fleming and S.O.R. Moheimani, *Passive vibration control via electromagnetic shunt damping*, IEEE/ASME Transactions on Mechatronics, Volume 10, Number 1, pp.118-122, March 2005.

[6]. C. Paulitsch, P. Gardonio and S.J. Elliott, *Active vibration damping using an inertial, self-sensing, electrodynamic actuator*, proceeding ASME 2005 International Design Engineering Technical Conferences & Computers and Information in Engineering Conference, New York.

[7]. F.C. Wang and W.J. Su, 2007, *The Impact of Inerter Nonlinearities on Vehicle Suspension Control*, accepted, to appear in Vehicle System Dynamics.

[8]. F.C. Wang, C.H. Yu, M.L. Chang and M.S. Hsu, 2006, December, *The Performance Improvements of Train Suspension Systems with Inerters*, Proceedings of the 45th IEEE Conference on Decision and Control, pp. 1472-1477, San Diego, CA, USA.